

RSC Advances



This is an *Accepted Manuscript*, which has been through the Royal Society of Chemistry peer review process and has been accepted for publication.

Accepted Manuscripts are published online shortly after acceptance, before technical editing, formatting and proof reading. Using this free service, authors can make their results available to the community, in citable form, before we publish the edited article. This *Accepted Manuscript* will be replaced by the edited, formatted and paginated article as soon as this is available.

You can find more information about *Accepted Manuscripts* in the [Information for Authors](#).

Please note that technical editing may introduce minor changes to the text and/or graphics, which may alter content. The journal's standard [Terms & Conditions](#) and the [Ethical guidelines](#) still apply. In no event shall the Royal Society of Chemistry be held responsible for any errors or omissions in this *Accepted Manuscript* or any consequences arising from the use of any information it contains.

Cite this: DOI: 10.1039/c0xx00000x

www.rsc.org/xxxxxx

ARTICLE TYPE

Unusual morphologies of reduced graphene oxide and polyaniline nanofibers-reduced graphene oxide composites for high performance supercapacitor applications

Rahul S.Diggikar^a, Dattatray J. Late^c, and Bharat B. Kale^{*b}

5 Received (in XXX, XXX) XthXXXXXXXXXX 20XX, Accepted Xth XXXXXXXXXXXX 20XX
DOI: 10.1039/b000000x

Herein, we have demonstrated the nanostructured rose flowers, sheets, rods and ferns of reduced graphene oxide by using oxalic acid as a reducing agent. The various morphologies of reduced graphene oxide were obtained by time dependent reduction of graphene oxide. The composites of reduced graphene oxide based polyaniline nanofibers, flower bouquet, and honeycombs were grown at a moderate temperature (60⁰C) by *in situ* polymerization of aniline. The structural characterization of composites was performed by using X-ray diffraction, and the existence of reduced graphene oxide in different size, shape and thickness confirmed by Raman spectroscopy and transmission electron microscopy study. The electrochemical study of reduced graphene oxides and their composites with polyaniline nanostructures was performed. The composite of honeycomb reduced graphene oxide – polyaniline nanofibers showed enhancement in the electrochemical performance (specific capacitance: 470 Fg⁻¹) compared to earlier reports. Such type of composites will be the potential contender for super capacitor.

Keywords: Reduced graphene oxide, morphology, polyaniline, composites

1. Introduction

20 Reduced graphene oxide (RGO) has been synthesized using a simple chemical method which has potential applications in various nano-electronics devices. Many methods have been reported for the preparation of the RGO, such as lithography, sonochemical, chemical vapour deposition (CVD) methods etc.¹ Controlled morphology of RGO has not yet been well studied due to different process parameters and steps involved in the synthesis. The CVD is one of the most popular, powerful and well controlled method to synthesize desired morphology and structures of graphene and / RGO.^{1-8,8a} But, the problem yet unresolved with CVD; yields poor quality of RGO and also shows low electrochemical performances.^{3,5,9} Chemical methods were found to be economical and effective for producing RGO in large scale. Therefore, chemical methods are more suitable for synthesizing high-performance RGO and RGO based composites.¹⁰ Challenge of preparation of highly crystalline and excellent quality with a large area single sheets of RGO has not yet been resolved.² However, the reduction of graphene oxide (GO) to RGO is not efficient by using hydrazine hydrate as a reducing agent. It is known that, the hydrazine hydrate is toxic, carcinogenic and unstable. Hence, it is necessary to investigate highly efficient, low toxic and eco-friendly reducing agent for the synthesis of the RGO.¹¹ In view of this, we synthesized highly populated nanorose flower,

nanorods, nanoferns and nanosheets of RGO in various interesting morphologies from GO. Such unique morphologies of RGO from GO have been demonstrated for the first time by simple chemical treatment. The chemical treatment is more efficient for the production of RGO which was further used for the synthesis of RGO based polyaniline composites.⁶ Very recently, Niu *et al*^{11a} presented the RGO-polyaniline composite which shows better electrochemical property than platinum (Pt) alone. Xiong *et al*^{11b}, Xia *et al*^{11c}, Tan *et al*^{11d} and Yu *et al*^{11e} presented the different polyaniline based metal oxides, RGO ternary nanocomposite with enhanced electrochemical performance. Wang *et al*^{11f} presented the PEDOT (polyethylene dioxythiophene) based metals; RGO ternary nanocomposite for supercapacitor. Dong *et al*^{11g} presented the RGO alone for supercapacitor. In some reports the polyaniline based RGO composites are also used as a separator in super capacitor and pollutant remover. In the ternary composite of RGO restricts use in device application because of transport of electron. The metal or binary metal oxide based polyaniline composite are expensive. The RGO alone cannot be used because of low conductivity which depends on size of layer. The major drawback of use RGO in supercapacitor is the tendency of restacking, agglomeration.^{11h} Metal oxides like RuO₂ are costly and polyaniline has the problem of stability in electrochemical performances. The RGO and polyaniline shows the weak interaction in composites, therefore, it restricts the applications for super capacitor.^{12, 12a}

In this context, the composites of RGO-polyaniline with strong interaction in different morphologies are synthesized by *insitu* polymerization by using mild oxalic acid (O.A.) The O.A. plays important role i.e. reduction of GO in controlled morphology and form acidic environment for the polymerization of aniline. As morphology changes the properties like conductivity and capacitance also changes. The size, shape and thickness of RGO are important for various applications. The desired size, shape and thickness of RGO can only be achieved by using a surfactant, it is demonstrated the same without surfactant.^{12b} Presented chemical approach and *insitu* polymerization gives RGO and RGO –polyaniline composites structures in desired shape, size and dimensions for primary and realistic applications. The nanostructures of RGO and RGO polyaniline nanocomposite synthesized by acidity and temperature dependent.^{12a} However, time dependent synthesis of nanostructures are presented herewith.

2. Experimental section:

2.1 Materials

Graphite powder was obtained from Carbon Ever flow Ltd. Concentrated sulfuric acid (H_2SO_4) (98%), potassium permanganate ($KMnO_4$), sodium nitrate ($NaNO_3$), oxalic acid (O.A.), ammonium persulfate (A.P.S.), Aniline, hydrogen peroxide (H_2O_2), hydrochloric acid (HCl) were purchased from S D Fine Chem. company used as received.

2.2 Synthesis of polyaniline nanofibers

The polyaniline nanofibers were manufactured by chemical oxidative polymerization of aniline in an acidic solution containing 1.5 M O.A. Polymerization was initiated by drop wise addition of oxidizing agent ammonium persulfate (A.P.S.) to the acidified solution containing the aniline at 0-10°C temperature under continuous stirring. After completion of the polymerization, the stirring was kept for 36 hrs at room temperature. The final product was filtered, washed and dried. During filtration a colourless filtrate was obtained is the confirmation of complete polymerization. A free flowing powder of the polymer was obtained and subjected to the characterization.

2.3 Synthesis of GO

GO was synthesized from graphite powder by a modified Hummers method.²⁷ In a typical synthesis, 1.0 gm of graphite and 0.5 gm of $NaNO_3$ were mixed in 25 ml concentrated H_2SO_4 (98%) in a 100 ml flask. The mixture was stirred for 30 minutes (min) in ice bath. While maintaining vigorous stirring, 3.0 gm of $KMnO_4$ was added to the mixture, the temperature was maintained ~20°C for overnight. As the reaction progressed, the mixture gradually became pasty and the colour turned into light brownish. Further, 30 ml of water was slowly added to the paste with vigorous agitation. The reaction temperature was rapidly increased up to 90°C and the colour changed to yellow. The aqueous suspension was stirred at 90°C for 24hrs. Then, 10 ml of 30% H_2O_2 was added to the mixture. For purification, the mixture was washed by rinsing and centrifugation (9000 revolutions per minute (rpm) for 30 min) with 5% HCl and deionised water (DI)

for several times. The product was evaporated and obtained GO.

2.4 Synthesis of nanosheets, nanorose flowers, nanorods, and nanoferns of RGO

7.0 gm of O.A. dissolved in 90 ml DI. To this, 10 ml GO suspension (4.1 mg ml^{-1}) was added. The solution was stirred vigorously for 2hrs at 60°C. The product was filtered and washed with DI by several times and dried. The same procedure was used for the synthesis of RGO nanostructures at 4, 6 and 12 hrs. The products were filtered and washed with DI several times and dried. The nanosheets of RGO were further used for the synthesis of RGO –polyaniline nanocomposites.

The nanosheet, nanorose flowers, nanorods and nanoferns of RGO are obtained at 2, 4, 6 and 12hrs respectively.

2.5 Synthesis of RGO – polyaniline nanofibers hierarchical composites

Among various nanostructures of RGO obtained in section 2.4, nanosheets of RGO (2.0 mg) were dispersed in 100 ml 3% O.A. solution by vigorous stirring. Aniline with 100% weight percentage of RGO nanosheets were slowly injected into above solution during magnetic stirring. After 2hrs, APS with 1:1 mole ratio of monomer was then added to the solution. The mixture was allowed to react for another 2hrs under constant stirring. The resulting product was filtered and washed with DI and dried. The same procedure was used for the synthesis of RGO - polyaniline nanocomposite at 8 and 12hrs.

The nanocomposites of RGO nanosheets -polyaniline nanofibers composite, flower bouquet and honeycomb RGO - polyaniline composites are obtained at 4, 8 and 12hrs respectively.

2.6 Characterizations

The crystallographic structures of the RGO – polyaniline nanofibers hierarchical composites and RGO were determined by X-ray diffraction (XRD, Bruker D8-diffractometer) equipped with a Cu K α radiation ($\lambda=1.544\text{Å}$). The initial changes on the surface as well as the coating of polyaniline nanofibers on RGO were recorded by Fourier Transformed Infrared Spectrophotometer (FT-IR, SHIMADZU 8300) in the range of 2000-800 cm^{-1} . Raman spectra for the honeycomb RGO - polyaniline nanofibers composite and RGO were obtained with a micro-Raman system. Microstructures and structural morphologies of the hybrids were investigated by Field Emission Scanning Electron Microscopy (FE-SEM, Hitachi S-4800) and High Resolution Transmission Electron Microscope (HR-TEM, JEOL-2010). Brunauer, Emmett, Teller (BET) method is used for surface area analysis of honeycomb RGO-polyaniline nanofibers composite. Hierarchical RGO-polyaniline nanofibers composites and RGO pressed into tablets under a hydraulic press to mirror finishing were subjected to the standard four point probe method for conductivity measurements. The polyaniline nanofibers were also characterized by XRD. For centrifugation used Remi Micro Centrifuge Model RM-12C/12CDX.

2.7 Electrochemical studies

The electrochemical measurements were carried out using an Auto lab PGSTAT30 (Eco Chemie) Potentiostat / Galvanostat employing a standard three-electrode electrochemical cell which

consisted of a composite loaded glassy carbon as the working electrode, an Ag/AgCl as the reference electrode, and platinum gauze as the counter electrode. Glassy carbon electrodes (GCE) of 3.0 mm in diameter were polished with finer emery-paper and 0.3 μm Al_2O_3 powder. This working electrode was cleaned in an ultrasonic bath for 1 min and dried under the IR lamp. In a typical process for all composites loading, composites were dispersed in N-Methyl pyrrolidone (NMP) with 0.2 ml of Nafion solution and sonicated in an ultrasonic bath for 5 min to get a homogenous solution. Then, about 10-20 μL of the mixture was coated on GCE and dried in air at 60°C for 5 min. Electrochemical experiments were carried out at room temperature in 1M aqueous H_2SO_4 solution as the electrolyte. All potentials are reported relative to an Ag/AgCl (sat. KCl) reference electrode at different scan rates and the potential window for cycling were confined between -0.1V and 0.8V. The same system was used for the electrochemical impedance measurements (EIS).

3 Results and Discussion:

It has been well studied that the O.A. acts as a reducing agent for GO^{12, 13} and also act as a dopant for aniline polymerization, which further improves the solubility of polyaniline composites. Further, it reduces the impurities and most importantly it helps to coating of polyaniline on RGO.¹³⁻¹⁶

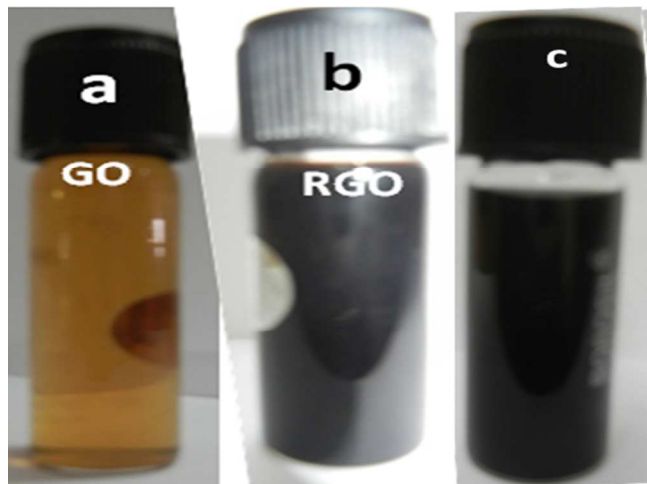


Fig.1: Photographs of suspension of (a) GO (b) RGO (c) Honeycomb RGO-polyaniline nanofibers composite

The synthesis scheme of nanorose flowers, nanoferns, nanosheets, nanorods of RGO and composites of flower bouquet, nanosheets, honeycombs of RGO-polyaniline nanofibers are shown in Fig. 2 and the corresponding FESEM images are shown in Fig. 4

The direct chemical exfoliation, reduction of GO to RGO was carried out. Recent few reports describe the reduction of GO by O.A, ascorbic acid and silver at high temperature.^{12, 17,18} The reaction for reduction of GO of carboxylic acids is given below.



The RGO based polyaniline composites have been reported to the supercapacitor application and hence have been synthesized by *in*

situ polymerization using RGO and aniline.^{12, 27, 28}

The reactions involved in the synthesis of RGO and RGO-polyaniline nanofibers are given below.

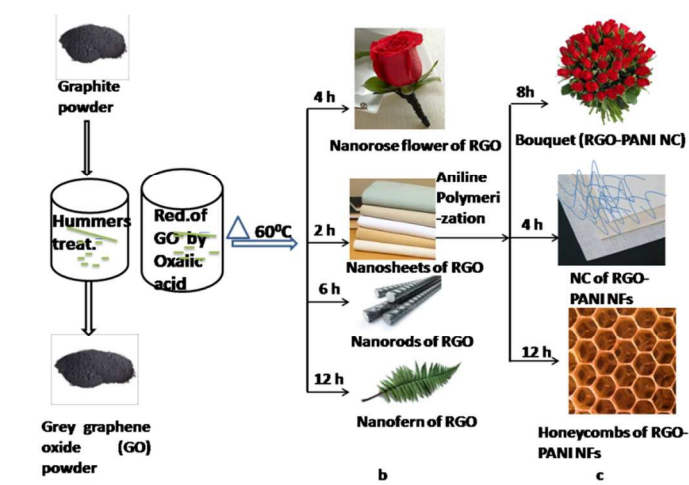
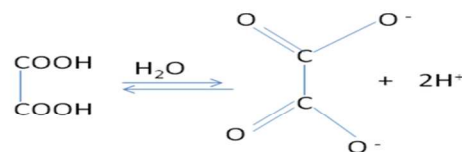


Fig.2:(a) Preparation of GO (b) RGO in the morphologies of (i) Nanorose flower (4hrs), (ii) Nanosheets (2hrs), (iii) Nanorods (6hrs), (iv) Nanoferns (12hrs) (c) Composites of (i) flower bouquet of RGO-polyaniline nanofibers (8h), (ii) nanosheets RGO-polyaniline nanofibers (4h), (iii) Honeycomb RGO- polyaniline nanofibers (12hrs).

Fig.4 reveals the FESEM images of RGO nanosheets, (a,b) nanorose flowers, (c,d) nanorods (e,f) nanoferns, (g,h) and composites of (i - l) RGO-polyaniline nanofibers in the form of flower bouquet (i,j), honeycombs RGO-polyaniline(k,l). These morphologies are quite interesting with size in the range of 0.5-10 μm . Such morphologies were obtained due to the mismatch of strain with GO and RGO during treatment. The effect of mismatch strain is considered, which predicts a strain induced instability under a compressive strain of GO and RGO under a tensile strain. Most interesting morphology formed were composites of honeycomb RGO with polyaniline nanofibers as shown in FESEM images Fig. 4(k, l) having larger sheet size.^{8,28} Novoselov *et al*^{28a} presented the honeycomb structure is atomic level; however, the structures in this report shown in FESEM / HRTEM are even to micro scale.

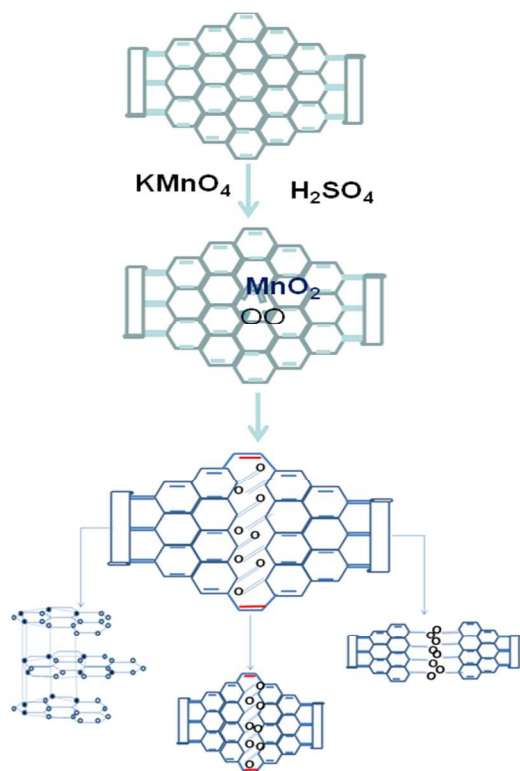


Fig.3: Schematic of functionalized RGO²⁹ Resulting in different morphology (Phenyl functionalized GO (Ph- GO) and GO can be thermally reduced. 4-iodophenyl functionalized GO (I-Ph-GO) can be thermo chemically reduced at 60 °C.)

Causes of different morphologies of RGO and RGO-polyaniline nanocomposites:

For the formation of different types of morphology of RGO and RGO-polyaniline based composites, the concentration of defects/edges were responsible caused by the effect of temperature and reaction time.³⁰⁻³³ It is observed that, the RGO nanosheets shows the less edges / defects due to the less chemical reaction time of 2hrs as shown in Fig. 4(a,b) As reaction time increases, the edges / defects along with population increases as depicted in FESEM image (Fig. 4). On treatment of GO with O. A. GO can be activated due to the rapid loss of oxygen and can be modulated for desired morphology.¹² However, plausible mechanism of formation of hierarchical nanostructures of RGO and RGO based composites in the presence of O.A. as shown in reactions [1-4] and Fig.3. The reaction of formation of magnate ester is the rate determining reaction, on further reducing alcohol can be formed.^{33,34} As the process continues, due to strains there is a chance to react the carbonyl group. Further, as the bond angle strain increases, the edges or defects in RGO nanosheets increases by which finally the honeycomb morphology was obtained.

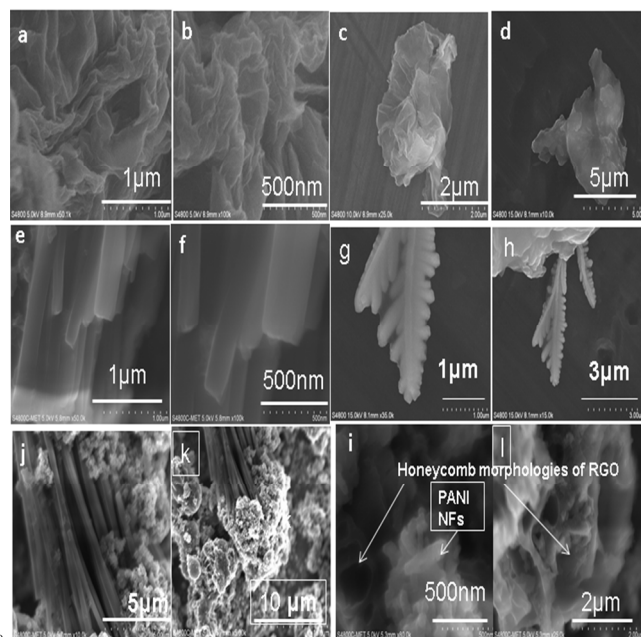


Fig. 4: FESEM images of nanosheets RGO (a-b), nanorose flower RGO (c-d) nanorods RGO (e-f), nanoflowers RGO (g-h), flower bouquet (RGO-polyaniline nanofibers composites) (i-j), and honeycombs of RGO-polyaniline nanofibers composites (k-l).

The morphology of nanorose flower and nanorods (Fig.4, c-f) is behave like a curling of RGO. However, the curling in RGO obtained by various treatment such as sonication due to capillary action. It is important that these morphologies of RGO can also be obtained in presence of O.A.^{33b} The fern morphology clearly indicate the suspension of RGO liquid crystals in the mesogenic state. In the mesogenic state of liquid crystals the solid state are always in orientational order with liquid phase. (Shown in S5, Fig.4g, h). It can be obtained by controlled treatment of GO.^{33a}

Fig.5 shows the TEM images of (a, b) RGO single layer nanosheets is one of the most common morphology,²⁷ (c, d) composites honeycombs RGO-polyaniline nanofibers (e, f) flower bouquet and (g, h) composites of RGO nanosheets-polyaniline nanofibers. In order to show the good crystallinity of the composites with periods of *in situ* polymerization in the present SAED pattern indicate the crystallinity in honeycomb RGO polyaniline composite is more. This is because of surface modification in the RGO and structure of polyaniline.²⁶ The well-defined diffraction spots in the corresponding SAED pattern indicated the multilayer structure of the as-prepared honeycomb RGO in honeycomb RGO-polyaniline nanofibers composite.¹² A comparison study discloses that the composites show an increasing of crystalline behaviour with *in situ* polymerization period honeycomb RGO-polyaniline composites >flower bouquet> composites of RGO nanosheets – polyaniline nanofibers. This also indicates the electrochemical performances and conductivity of RGO based composites depend with period of chemical treatment and the amount of polyaniline nanofibers coated on RGO shown later in this manuscript. The more amounts of polyaniline nanofibers are coated on RGO nanosheets as shown in (supplementary Information) S.I.1 its conductivity and capacitance is less as compared to other two RGO based composites.

Fig.5a presented the SAED pattern of hierarchical RGO-

polyaniline composites. Fig.5a (a) indicates the SAED pattern of RGO sheets – polyaniline composites which indicate the nature of composite is less crystalline, Fig.5a (b) SAED pattern of flower bouquet and Fig.5a(c) indicates the SAED pattern of honeycomb RGO-polyaniline composites. The good crystallinity is observed in Fig.5a(c). The crystallinity is higher due to the honeycomb RGO. This is also observed in XRD measurement. The intensity of 2theta peak at 25.1° is decreases in Fig. 6a demonstrated the quantity of PANI NFs and ultimately by crystallinity.

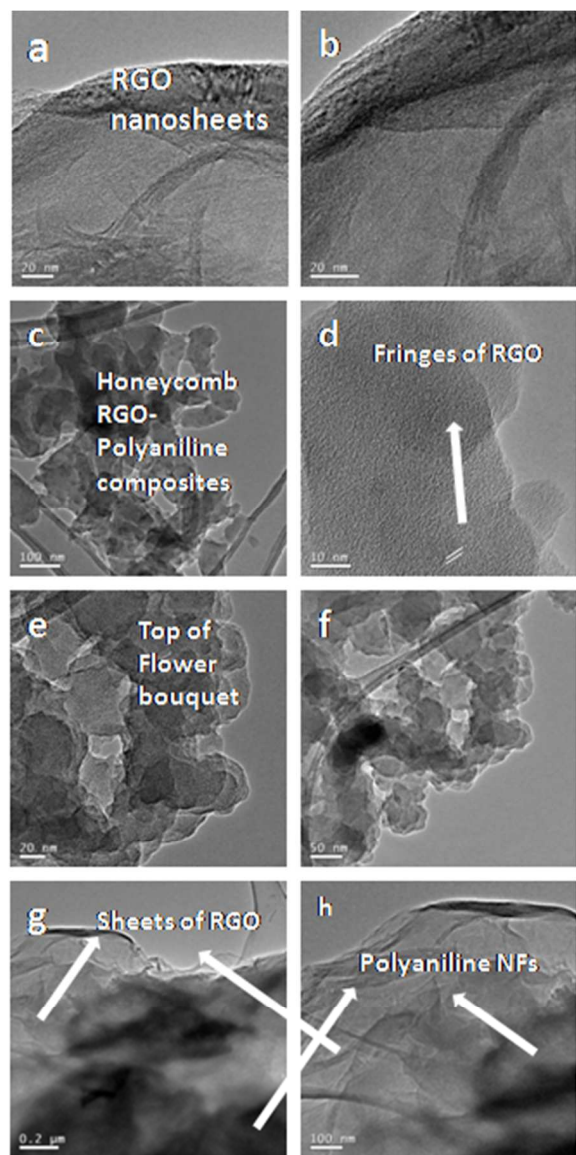


Fig. 5: TEM images of (a-b) Multilayers nanosheets of RGO, (c,d) Honeycombs of RGO-polyaniline composites, (e-f) flower bouquet-polyaniline nanofibers composite and (g,h) nanosheets RGO-polyaniline nanofibers composite.

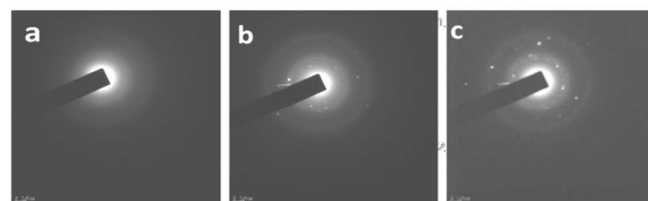


Fig.5a. SAED pattern of RGO nanosheets-polyaniline composites (a) flower bouquet (b) honeycomb RGO- polyaniline composites (c)

20 Morphological properties of the samples:

The incorporation of RGO in polyaniline was easily carried out by simple method. At lower current density the polyaniline gets degradation in the electrochemical performance, the RGO acts as the mount exertion to avoid cracking of polyaniline during cycling.^{12a}

The layered structure of RGO is shown in Fig. 4a,b. The TEM image (Fig.5a, b) showed lateral view of RGO sheets in several micrometers which are obtained after 2hrs treatment in O.A. When RGO sheets are treated with aniline monomers by *insitu* polymerization the polyaniline nanofibers are coated on the surface of RGO (RGO nanosheets- polyaniline nanofibers composite shown in S.I.1), tip of RGO rods (flower bouquet Fig.4 i,j, Fig.5 e,f) and coated / intercalate in RGO honeycomb (Fig. 4 k,l). The advantage of composite of polyaniline with RGO is clearly demonstrated that, the RGO allowed deposition to polyaniline nanofibers at every corner of the surface and the attachment between them.^{12c}

Fig. 6 reveals the XRD patterns (JCPDS 065-6212) of (c) RGO nanosheets, composites of (b) RGO-polyaniline nanofibers in the form of flower bouquet (a) honeycombs and (d) nanosheets. The XRD of RGO shows fairly intense peaks at $2\theta = 26.23$ and 43.3° ^{12a, 38, 38a-c} However, all composites show broad peaks at $2\theta = 20.0$ and 25.1° ascribed to polyaniline nanofibers. The broadness of peak indicates the amorphous nature of all composites (in respect of crystallinity to each other). However, the broadness is not same in the all peaks.^{22,34-40,41} The absence of RGO peak at $2\theta = 43.3^\circ$ clearly shows homogeneous formation of RGO-polyaniline nanofibers composites. It is noteworthy that the presence of weak peak at $2\theta = 6.34^\circ$ indicates polyaniline nanofibers in composites confirmed by XRD (S.I.2a.). From the XRD studies, RGO-polyaniline composites indicate that the RGO sheets are successfully exfoliated.

Fig. 7 reveals the FTIR study of RGO nanosheets and the hierarchical composites of RGO- polyaniline nanofibers. The featureless FT-IR spectrum of RGO indicates that the chemical reduction of GO is relatively complete (Fig. 7d). In case of all hierarchical RGO-polyaniline nanofibers composites Fig.7 (Fig. 7a- c) the characteristic bands at 1503 cm^{-1} ascribed to C=C stretching vibration in rings, whereas the bands $\sim 1100\text{-}1300\text{ cm}^{-1}$ were related to the RGO bonded with PANI NFs.^{12, 14, 40-45, 45a}

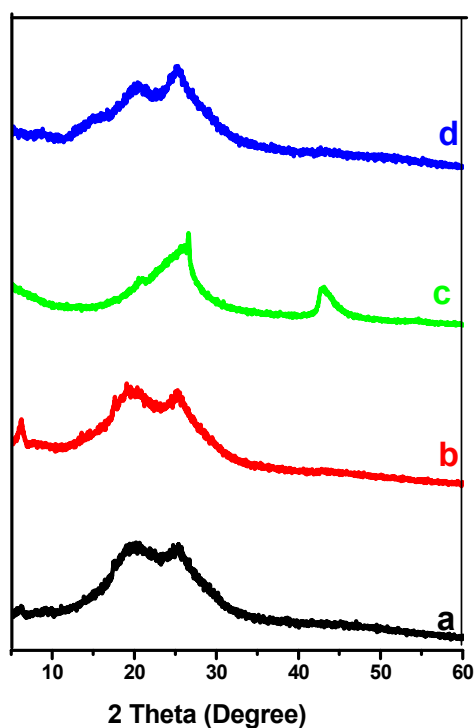
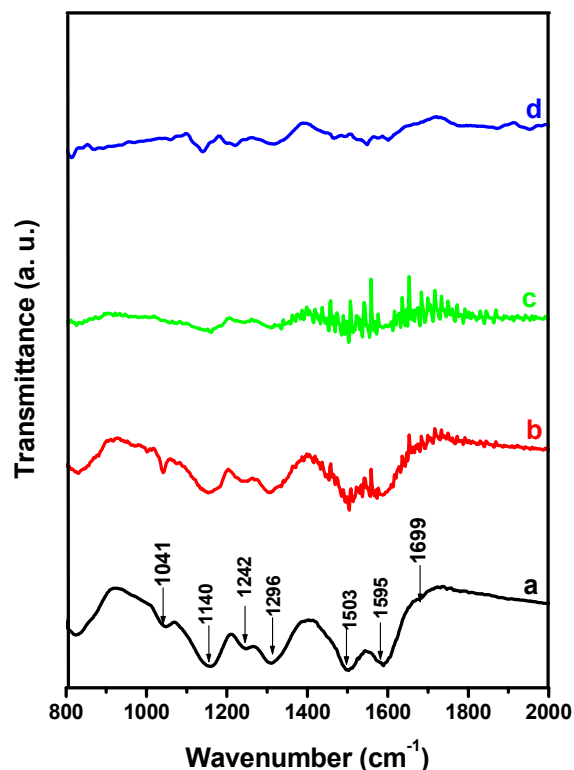


Fig. 6: XRD patterns of (a) Honeycomb RGO- polyaniline nanofibers composites (b)flower bouquet(c) RGO nanosheets (d) RGO nanosheets-polyaniline nanofibers composites

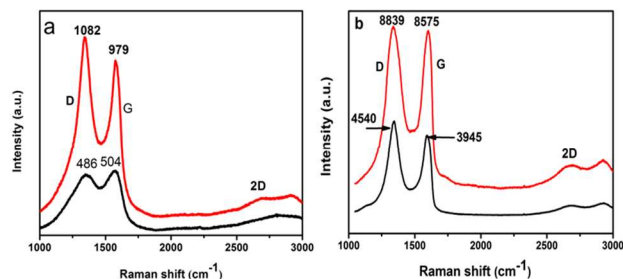
5 The presence of these bands suggests the successful coating of polyaniline nanofibers on RGO nanosheets and all above characteristic peaks strongly indicate the successful polymerization of polyaniline nanofibers in and on RGO. The increase in the intensity of the band at 1140 cm^{-1} was attributed to charge delocalization indicating that the interactions existed between RGO and polyaniline nanofibers.³⁹ The peaks observed at 1595 and 1699 cm^{-1} in doped polyaniline nanofibers are due to the carboxyl group may be originating from O.A.^{13, 42}

Fig.8 reveals the Raman study of RGO, RGO-polyaniline 15 nanofibers composites. The formation of layers / nature of RGO and its composites are well studied by various groups with the help of Raman spectroscopy. The intensity / formation of D, G and 2D peaks reveal the defects in RGO. However, intensity of D peak is less in RGO hence the defects are less (a) however more in honeycomb RGO- polyaniline nanofibers NC (b). The intensity of D peak is more than G peak in flower bouquet / honeycomb RGO- polyaniline nanofibers composites indicates the size. The 2D peak is shifting towards higher from RGO to honeycomb RGO-polyaniline nanofibers composite hence it is more 20 crystalline as it possesses pentagon / hexagon. Sanderson *et al*^{42a} presented the honeycomb RGO is a material of bendy displays. RGO with polyaniline gives more appropriateness for bendy displays.

Raman study is also useful for the understanding the thickness 30 of RGO. The D peak in all four samples indicates the RGO is present in all four samples. The existence of 2D peak in the samples revealed (a) the RGO is in single layer (b) thicker in size and (c) local effect caused disorder.



35 Fig.7: FTIR study of (a) Honeycomb RGO-polyaniline nanofibers composites (b) composites of flower bouquet (c) RGO nanosheets-polyaniline nanofibers composites (d) RGO nanosheets.



40 Fig.8 (a) Raman spectra of RGO (black spectra), flower bouquet (red), (b) nanosheets RGO- polyaniline nanofibers composites (black spectra) and honeycomb RGO- polyaniline nanofibers composites (red spectra)

Such effects are only observed in single layer at lower temperature. D band is characteristic of defects and disorders of chemically reduced graphene sheets.^{42h} It is mentioned earlier 45 about the intensity of D peak increases / decreases, in Fig. 9a the intensity of D peak is less due to the removal of hydrogen atom and defects bound to the basal plane of RGO.^{42b} This is not observed in composite because of protonation. The thickness of single layer RGO is less than reported elsewhere.^{42c} However, the 50 multilayer of RGO can be formed at higher temperature.^{42d} The minimum surface area indicates the RGO has been restacked and aggregated (S.I.4).^{11h, 42e, 43, 44.}

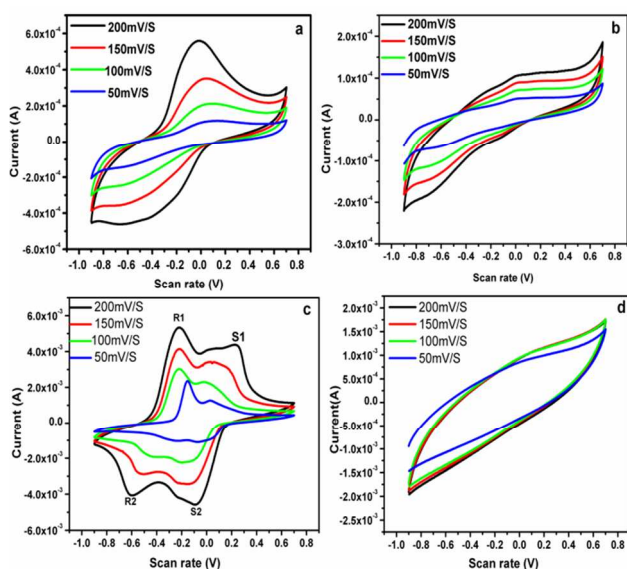


Fig.9.CV study of (a) Honeycomb RGO-polyaniline nanofibers composite (b) flower bouquet –polyaniline composite (c) Nanosheets RGO-polyaniline nanofibers composites and (d) RGO nanosheets

Fig.9 shows the electrochemical performances of the hierarchical RGO-polyaniline nanofibers composites and RGO nanosheets including its capacitive behaviour which were analyzed using a CV in 1M H₂SO₄ with a potential range of -0.1 and 0.8V versus Ag/AgCl at various scan rates (V). The capacitance estimated from the CV curve was reported by integrating over the CV to determine the average value of the area for one cycle. Remarkable difference of electrochemical surface activity among the RGO nanosheets (Fig.9 (d)) and the hierarchical RGO-polyaniline nanofibers composites is recorded at different scan rates can be easily recognized from the representative CV curves shown in Fig.9 (a-c).

When compared with the RGO electrode, the current density response and the CV loop area of the hierarchical RGO – polyaniline nanofibers composites electrodes are much larger than RGO. This indicates that the electrochemical performance of the hybrid is remarkably enhanced owing to the dependence of polyaniline nanofibers coating on the surface of the RGO sheets. Two pairs of well-defined redox peaks appeared for the hybrids, which were attributed to redox transitions of polyaniline nanofibers, suggesting the presence of pseudo capacitance of polyaniline nanofibers Fig.9(c).³⁶ These peaks correspond to the redox transitions between semiconducting states (the leucoemeraldine form) to a conducting state (polaronic emeraldine) designated as peaks R₁/S₁ and the Faradic transformation of emeraldine to pernigraniline initiates the redox peaks R₂/S₂(Fig.9(c)).¹⁸ It was observed that the cathodic peaks shift positively and the anodic peaks shift negatively with an increment of potentially sweep rates. As exhibited in Fig. 9(c), the CV curve of the RGO-polyaniline nanofibers composites is close to being rectangular shapes for all scan rates which indicates that the excellent electrical double-layer capacitance. Further, with the increasing sweep rate, increase of specific capacitance was observed.

Electrochemical mechanism and morphologies of PANI and RGO- PANI NFs nanocomposites

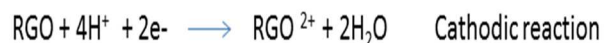
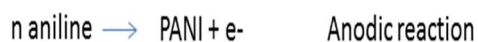
Wang *et al*^{45a} presented the electrochemical performance of PANI

and RGO-PANI NFs nanocomposites which depends on the morphology and interaction of PANI and RGO at the interfacial. The various morphologies of PANI and RGO-PANI NFs nanocomposites the electrochemical performance mechanism is explained in detail somewhere. However, the arrangement of PANI NFs on RGO are clearly demonstrated the ionic diffusion path for electrode materials.

The observed CV were quite stable for a number of cycles and no significant current decrease was noticed in all the cases, which clearly indicates the compound exhibited high cycling stability excluding RGO as shown in Fig. 9d . It can be seen that the CV curve of RGO exhibits (Fig.9d) only one pair of redox peaks due to the transition between quinone / hydroquinone states, which is typical for carbon materials with oxygen- functionalities.^{19,20} Therefore, there is no stability in the case of RGO, hence requires composites with polyaniline for stability. The CV curve is nearly rectangular in shape, indicating good charge propagation within the electrode; therefore, it is clearly proved that the loading of polyaniline nanofibers with RGO and the composite used for the electrode is more efficient. The rectangular CV shape of RGO (Fig. 9d) demonstrated electrical double layer capacitance ~ 100 Fg⁻¹ (obtained 150 Fg⁻¹, Table 1) on the other side in RGO-polyaniline composites it is enhanced upto 470 Fg⁻¹ due to combination of redox capacitance and electrical double layer capacitance.^{42c} From observations of Table 1 it is concluded that the conductivity and capacitance are depends on the surface modification of RGO and quantity of polyaniline on RGO. However, due to the issue of reduction of GO and absence of polyaniline it shows lower conductivity ultimately the lower change in current with different scan rate with Ohmic behaviour.^{42f}(Fig.9d, Table 1)

Cyclic voltammetry was also use to examine the heterogeneous electron transfer rate and interaction of the RGO with polyaniline nanofibers. We continued to probe the performances of hierarchical RGO- polyaniline nanofibers composites on their abilities to enhance the electron transfer kinetics, which play an important role in facilitating oxidation/reduction of molecules which require high overpotentials for oxidation/reduction. As such, the CV analysis was carried out on an important biomarker for all composites as shown in Fig.8. Honeycombs of RGO-polyaniline nanofibers composites showed the highest oxidation potential at 0.53V, followed by at 0.48V for composites of flower bouquet, composites of nanosheets of RGO –polyaniline nanofibers and the reduction potential ~ - 0.13V. Kim *et al*²¹ presented that the percentage of aniline (polyaniline) on RGO decides the conductivity and capacitance of composites. The utmost conductivity and capacitance is observed for honeycomb RGO-polyaniline nanofibers composites is maximum as compare to other it means the polyaniline nanofibers coating in honeycomb RGO is less (Table 1). This indicates that RGO produced with our method is suitable for electrochemical applications with improved performance.²²

The detailed electrochemical mechanism of PANI NFs- RGO nanocomposite is yet under investigation but the possible electrochemical mechanism is illustrated below^{22a,b}



The electrochemical impedance spectroscopy (EIS) data of RGO and hierarchical RGO-polyaniline nanofibers composites was analysed using Nyquist plots were shown in S.I.3 (a). The plots (the imaginary component (Z'') of the impedance against the real component (Z')) show the frequency response of the electrode / electrolyte system. The more vertical behaviour of the curve corresponds to a cell closer to an ideal capacitor.²⁶ As shown in S.I. 3 (a) Nyquist plots of RGO and hierarchical RGO-polyaniline nanofibers composites exhibits the data over the high frequency region, the low frequency region of honeycomb of RGO-polyaniline nanofibers composites. Large data point observed for these electrodes are indicative of high interfacial charge-transfer resistance.

Table1: Conductivity and capacitance study of RGO and RGO based composites

Serial Number	Composites	Conductivity (S/cm)	Specific capacitance (Fg^{-1})	Reference
1	Honeycomb of RGO- polyaniline nanofibers composites	204	470	Present work
2	Flower bouquet	157	230	Present work
3	RGO nanosheets - polyaniline nanofibers	154.9	210	Present work
4	RGO nanosheets	106	150	Present work
5	RGO nanosheets - polyaniline nanofibers	---	250	[39]
6	Polyaniline nanofibers		122	[42]
7	Polyaniline nonfibrillar	2-10	33	[42]
8	Silver vanadium oxide-polyaniline composites	----	365.5	[45]
9	Silver-Lithium vanadium oxide composites	----	124	[46]
10	Reduced Graphene Oxide	----	86-152	[47]
11	Graphene based supercapacitor		75	[48]

This is attributed to the electrical conductivity of these materials. The sloping portions of the Nyquist plots are the Warburg resistance resulting from the frequency dependence of ion diffusion / transport in the electrolyte. The larger Warburg region of these electrodes indicates greater variations in ion diffusion path lengths and increased obstruction of ion movement.

According to the Nyquist plot, all composites excluding RGO

nanosheets-polyaniline nanofibers shows vertical sloping curves suggests that interfacial charge-transfer is significantly low. However, RGO nanosheets-polyaniline nanofibers semicircle at high frequency is detected.

This indicates that interfacial charge transfer resistance of RGO honeycombs / flower bouquet polyaniline nanofibers composites is low and in case of RGO nanosheets-polyaniline nanofibers is high. Among the composites RGO honeycombs - polyaniline nanofibers composites indicates charge transfer significantly low because of the high conductivity which may be due to attributed to the honeycombs structure and low content of polyaniline nanofibers. However, there may be high content of polyaniline nanofibers in case of RGO nanosheets polyaniline nanofibers composites that is responsible for high interfacial charge transfer resistance and low conductivity. Except for the low electrical resistance, RGO honeycomb - polyaniline composites also exhibit short and the equal diffusion path length of the ions in the electrolyte; this can be seen from the neglectable Warburg region on the Nyquist plots. This may be because of the unique morphology of RGO honeycomb-polyaniline nanofibers composites.²⁸ It is quite possible that a small amount of polyaniline nanofibers in this composite are distributed homogeneously on the surface of honeycomb structured RGO. A similar phenomenon is observed in composites of flower bouquet, but less as compare to honeycomb structured RGO composites.²⁶

The capacitance of conducting polymers is an important factor to select the suitable material for supercapacitor. Wang *et al*³⁵ reported that the polyaniline nanofibers composites demonstrated the good capacitive behaviour and charge / discharge property. However, the behaviour of polyaniline nanofibers as like honeycombs of RGO-polyaniline nanofibers composite is able to meliorate this situation. The electrochemical stability of honeycombs of RGO-polyaniline nanofibers composites and RGO, nanosheet of RGO-polyaniline nanofibers were examined in 1M H_2SO_4 aqueous electrolyte by consecutive charge- discharge cycles at a current density of 1Ag^{-1} . S.I.-3(b) shows the charge/discharge curves of hierarchical NC of RGO-polyaniline nanofibers and honeycomb-polyaniline nanofibers composites. All curves exhibit equilateral triangle shape, featuring that the potential of charge/ discharge is a linear response to them, indicating a good reversibility during the charge/discharge processes. The specific capacitances of all composite along with earlier report have been summarized in Table 1. It is noteworthy that utmost specific capacitance (470Fg^{-1}) is obtained for the honeycomb RGO- polyaniline nanofibers composites. The decrease specific capacitance of other composites ascribed to the change electronic structure and morphology of the composites. The higher capacitance observed for honeycomb RGO-polyaniline nanofibers composites is due to low interfacial charge transfer resistance as stated in impedance analysis due to unique morphology and homogeneous distribution of polyaniline nanofibers in composites.

From the Table1 it concludes that there is synergic effect of morphology on the electrochemical behaviour of the composites. The further works is necessary to improve the morphology of RGO composites for better capacitance. The change in morphology changes the properties and hence the

applications⁴⁹ further study of honeycomb structured RGO is in progress.

Conclusions

We have demonstrated unique morphologies of RGO and RGO based polyaniline nanofibers composites. We have synthesized nanorose flowers, nanoferns (dendrites), nanosheets and nanorods of the RGO. Further we found that the *insitu* polymerization of aniline with RGO gives unique morphologies of composites. The morphology likes flower bouquet; honeycombs for RGO-polyaniline nanofibers composites have been demonstrated. The large size single sheets of RGO in the range of 0.5-10 μm were obtained by using nontoxic, economical, eco-friendly and water soluble organic acid. We observed enhanced specific capacitance (470 Fg^{-1}) and conductivity (204 Scm^{-1}) for honeycomb like RGO-polyaniline nanofibers composites. We are very curious to investigate the further properties of this honeycomb structure that is in progress.

Acknowledgments

One of the authors RSD would like to thank UGC, New Delhi (File No. 34-34/08) for granting Teacher Fellowship, and Ahmednagar Jilha Maratha Vidya Prasarak Samaj, Ahmednagar (one of the reputed educational institutes in India) and C-MET, Pune,

Notes and References

^aPost Graduate Department and Research Centre in Chemistry, New Arts, Commerce and Science College, PARNER - 414302 Ahmednagar (M.S.) India

^bCentre For Materials For Electronics Technology (C-MET) off Pashan Road, Pune- 411007 India
E-mail: kbbb1@yahoo.com

^cNational Chemical Laboratory, Pune, India

Supplementary Information (ESI): 1. FESEM study of RGO nanosheets - polyaniline nanofibers composites. 2. XRD study of polyaniline nanofibers. 3. Impedance and Nyquist plot. 4. BET surface area measurement of honeycomb RGO- polyaniline composites. 5. Liquid crystal of RGO

- M. A Rafiee, W. Lu, A. V. Thomas, A. Zandiatashbar, J. Rafiee, J. M. Tour, N. A. Koratkar., *ASC Nano*, 2010, **12**, 7415,
- X. Li, C. W. Magnuson, A. Venugopal, R. M., Tromp, J. B. Hannon, E. M. Vogel., L. Colombo., R. S., Ruoff *J. Am. Chem. Soc.* 2011, **133**, 2816,
- A. C. Dale, Brownson, C. E. Banks., *RSC Adv.*, 2012, **2** 5385,
- L. Jiao., L. Zhang, X. Wang, G. Diankov, H. Dai, *Nature*, 2009, **458**, 877.
- Y. A., Wu, Y. Fan, S. Speller, G. L. Creeth., J. T. Sadowski., K. He, A. W. Robertson, C. S. Allen, J. H. Warner, *ASC Nano*, 2012, **6**, 5010,
- M. A. Rafiee, J. Rafiee, Z., Wang, H. Song, Z. Z., Yu N. Koratkar, *ASC Nano*, 2009, **12**, 3884.
- N. Petrone, C. R. Dean, I. Meric, vander, A. M. Zande, P. Y., Huang, L. Wang, D. Muller, K. L. Shepard., J. Hone, *Nano Lett.* 2012, **12**, 2751
- Y. Zhang, L. Zhang, P. Kim, M. Ge, Z. Li, C. Zhou, *Nano Lett.* 2012, **12**, 2810 (a) H. Ma., P. Gao, D. Fan, B. Du, J. Hao, Q. Wei, *New J. Chem.*, 2013, **37**, 1307 (b) S. Park, Ji Won Suk,

- An, J. Oh, S. Lee, W. Lee, J. R. Potts, J. H. Byun, R. S. Ruoff *Carbon*, 2012, **50**, 4573 (c) J. Chen, H. Bi, S. Sun, Y. Tang., W. Zhao, T. Lin, D. Wan, F. Huang, X. Zhou, X. Xie, M. Jiang *ACS Appl. Mater. Interfaces*, 2013, **5** 1408
- A. S., Khojin, D. Estrada, K. Y. Lin., M. H., Bae, F., Xiong, E., Pop, R. I. Masel, *Adv. Mater.* 2012., **24**, 53
- H. Bai, C. Li, G. Shi, *Adv. Mater.* 2011, **23**, 1089,
- Y. Huang, Y. Chen, C. Hu, B. Zhang, T. Shen, X. Chen, M. Q. Zhanga, *J. Mater. Chem.*, 2012, **22**, 10999. (a) H. Niu, S. Zhang., Q. Ma, S. Qin, L. Wan, J. Xu, S. Miao, *RSC Adv.* 2013, **3**, 17228 (b) P. Xiong, H. Huang, X. Wang *Journal of Power Sources* 2014, **245**, 937 (c) X. Xia, Q. Hao., W. Lei, W. Wang, D. Sun, X. Wang *Journal of Materials of Chemistry*, 2012, **22**, 16844 (d) Q. Tan, Y. Xu, J. Yang, L. Qiu, Y. Chen, X. Chen *Electrochimica Acta* 2013, **88** 526 (e) G. Yu, L. Hu, N. Liu, H. Wang, M. Vosgueritchian, Y. Yang, Y. Cui, Z. Bao, *Nano Lett.* 2011, **11**, 4438 (f) W. Wang, W. Lei, T. Yao, X. Xia, W. Huang, Q. Hao, X. Wang, *Electrochimica Acta* 2013, **108**, 118 (g) L. Dong, Z. Chen, D. Yang, H. Lu, *RSC Adv.*, 2013, **3**, 21183 (h) Y. Wang, Y. Wu, Y. Huang, F. Zhang, X. Yang, Y. Ma., Y. Chen *J. Phys. Chem. C* 2011, **115**, 23192
- P. Song, X. Zhang, M. Sun, X. Cui, Y. Lin., *RSC Advances*, 2012, **2**, 1168. (a) Y. F. Huang, C. W. Lin, *Polymer*, 2012, **53**, 2574 (b) L. Zhang, S. Zhao, X. N. Tian, A. S. Zhao, *Langmuir*, 2010, **26**, 17624 (c) K. S. Kim, Y. Zhao, H. Jang, S. Y. Lee, J. M. Kim, K. S. Kim, J. H. Ahn, P. Kim, J. Y. Choi, B. H. Hong, *Nature*, 2009, **457**, 706
- E. Erdem, M. SaCak, M. Karakiqla, *Poly. Int.*, 1996, **39**, 153.
- Graphene oxide characterization sheet *NanoInnova Technologies* 7, 28049
- R. Rajagopalan, J. O. Iroh, *Electro. Acta*, 2001, **46**, 2443.
- H. A. Becerril, J. Mao, Z. Liu, R. M. Stoltenberg., Z. Bao, Y. Chen, *ACS Nano*, 2008, **2**, 463.
- H. Chen, M. B. Muller., K. J. Gilmore., G. G. Wallace., D. Li, *Adv. Mater.* 2008, **20**, 3557.
- J. Zhang, H. Yang, G. Shen, P. Cheng, J. Zhang, S. Guo, *Chem. Commun.*, 2010, **46**, 1112.
- D. R. Dreyer, S. Park, C. W. Bielawski, R. S. Ruoff, *Chem. Soc. Rev.*, 2010, **39**, 228.
- J. Shen, M. Shi, B., Yan H. Ma, N. Li, M. Ye., *J. Mater. Chem.*, 2011, **21**, 7795.
- J. Kim, S. J. Park, S. Kim, *Carbon Letters* 2013, **14**, 51
- X. Zhao, Q. Zhang, D. Chen, *Macromolecules* 2010, **43**, 2357. (a) L. Pani, H. Qiu, C. Dou, Y. Li, L. Pu, J. Xu, Y. Shi, *Int. J. Mol. Sci.* 2010, **11**, 2636 (b) R. Diggikar, J. Ambekar, M. Kulkarni, B. Kale, *New J. of Chem.* 2013, **37**, 3236
- D. V. Kosynkin, A. L. Higginbotham., A. Sinitiskii, J. R., Lomeda Dimiev A., B. K. Price., J. M., Tour *Nature*, 2009, **458**, 872
- L. Jiao, X. Wang, G. Diankov, H., Wang, H. Dai, *Nature Nanotechnology*, 2010, **5**, 321.
- F. O. Yang, B. Huang, Z. Li, J. Xiao, H. Wang, H., J. Xu. *Phys. Chem. C*, 2008, **112**, 12003
- K. Zhang, L. Zhang., X. S., Zhao, J. Wu, *Chem. Mater.* 2010, **22**, 1392.
- W. S. Hummers, R. E. Offeman, *J. Am. Chem. Soc.* 1958, **80**, 1339
- Y. Zhu, S. Murali, W. Cai, X. Li, J. Suk., J. R., Potts, R. S., Ruoff *Adv. Mater.* 2010, **22**, 3906. (a) K. S. Novoselov, A. K. Geim, S. V. Morozov, D. Jiang, Y. Zhang, S. V. Dubonos, I. V. Grigorieva, A. A. Firsov, *Science*, 2004, **306**, 666 (b) Q. Tang, Z. Zhou, Z. Chen, *Nanoscale*, 2013, **5**, 4541
- A. L. Higginbotham., D. V. Kosynkin, A. Sinitiskii, Z. Z. Sun., J. M., Tour, *ACS Nano*, 2010, **4**, 2059
- A. Mathkar, D. Tozier, P. Cox, P. Ong., C. Galande, K. Balakrishnan, A. L. Mohana Reddy, P. M., Ajayan *J. Phys. Chem. Lett.*, 2012, **3**, 986.
- X. Jia, J. Campos-Delgado, M. Terrones, Meunier V., Dresselhaus M. S., *Nanoscale*, 2011, **3**, 86
- M., Terrones. *ACS Nano*, 2010, **4**, 1775.

33. C.Bao, L.Song, W.Xing, B.Yuan, C. A. Wilkie, J.Huang, Guoa Y., Y.Hu, *J. Mater. Chem.*, 2012, **22**, 6088, (a) V. B. Shenoy, C. Damodara Reddy, Y.W.Zhang *ACS Nano* , 2010,**4**,4840 (b).N. Behabtu,J.R. Lomeda, M. J. Green,A. L. Higginbotham,A.Sinitiskii, D.V. Kosynkin, D.Tsentelovich, A. N.G. Parra-Vasquez,J.Schmidt, E. Kesselman, Y. C.Yeshayahu, Talmon J, M. Tour, M. Pasquali,*Nature Nanotechnology*, 2010,**5**,406
34. O. K.Park, M. G., Hahm S.Lee, H. I.Joh, S. I.Na, Vajtai R., Lee J. H., Ku B. C., Ajayan P. M.,*Nano Lett.*, 2012, **12**, 1789
35. G Wang,J.Yang, J.Park, X.Gou, B Wang,H.Liu, J. Y.Facile, *J. Phys. Chem. C*, 2008, **112**, 8192.
36. X.Rui, J.Zhu, D., Sim,C.Xu, Zeng Y., Hng., T. M., Lim Yanade Q., *Nanoscale*, 2011, **3** 4752
37. N. A., Kotov Dekany I., Fendler J. H., *Adv. Mater.* 1996, **8**, 637 ;
38. J. Li, *Nanostructured Biomaterials*,Springer,e-IISN, 1995,**6827** 115(a) S. Zhou, H. Zhang, Q. Zhao, X.Wang, J.Li, F. Wang, Carbon, 2013, 440 (b) S.Dubin,S.Gilje, K. Wang,V.C.Tung,K.Cha,A.S.Hall,J.Farrar,R.Varshneya,Y.Y ang, Ri. B. Kaner *ACS Nano* . 2010,**4**,3845(c)*R.Kurapati , A. M. Raichur. Chem. Commun.*, 2012,**48**, 6013
39. Y. S.Yang, M. X.Wan, *J. Mater.Chem*, 2002, **12**, 897
40. S.Lefrant, M.Baibarac, Baltog I.,*Mater. Chem.*, 2009,**19**, 5690
41. J.Zhang, X. S., Zhao *J. Phys.Chem.C* 2012, **116**, 5420.
42. X.Zhang, W. J.Goux, S. K.Manohar*J. Am. Chem. Soc.*, 2004, **126**, 4502. (a) K.S.Kim, Y. Zhao, H. Jang, S. Y. Lee, J. M. Kim, K. S. Kim, J.H.Ahn,P. Kim, J.Y. Choi,B. H. Hong, *Nature Letters*,2009, **457**, 706 (b)S.Ryu, J. Maultsch Melinda, Y. Han, P. Kim, L.E. Brus *ASC Nano*,2011, **5**,4123 (c)A. Vadivel Murugan, T. Muraliganth,A. Manthiram *Chem. Mater.* 2009, **21**, 5004(d)L.Liu,S.Ryu,M.R.Tomasik, E.Stolyarova,N. Jung, M. S. Hybertsen3, M. L. Steigerwald, L. E. Brus, G. W.Flynn, *Nano Lett.*, 2008, **8**, 1965 (e) Y. Sun, D.Shao, C.Chen, S. Yang, . X. Wang, *Enivornmental Science and Technology*, 2013, **47**, 9904 (f) S. Stankovich, D.A.Dakin, R.D.Pinar, K.A.Kohlhaas, A. Kleinhammes, Y. Jia, Y. Wu, S.T.Nguyen, R.S.Ruoff, *Carbon*, 2007,**45**, 1558 (h)*T. Kuila, S. Bose, A. K.Mishra, P. Khanra, N.H. Kim, J.H. Lee**Progress in Materials Science* **2012**,**57**, 1061
43. A.Salehi-Khojin., D.Estrada, K. Y Lin., M.H., Bae Xiong F., Pop E., Masel R. I. *Adv. Mater.* 2012, **24**, 53
44. A. C., Ferrari, *Solid State Communications* 2007, **143**, 47
45. R.S.Diggikar, M.V Kulkarni., G.M Kale., B.B Kale.,*J. Mater. Che.-A*, 2013, **1**, 3992(a) L.Wang, Y.Ye, X. Lu, Z.Wen, Z. Li, H. Hou, Y.Song, *Scientific Report*, 2013, **3**, .3568
46. R.S Diggikar., V.M., Dhavale,D.B Shinde., M.V Kulkarni., B.B.Kale *RSC Adv.* 2012,**2**,3231
47. S.Park, J.W Suk, J An., J. Oh S Lee. W Lee., J.R Potts. J.H., Byun ,R. S. Ruoff *Carbon*, 2012,**50**, 4573
48. S R C, Vivekchand, C. S.Rout.,K S Subrahmanyam, A, Govindraj, C N R, Rao *J.Chem.Sci.*, 2008, **120**, 9
49. D.H. Cho, L. Wang, J.S. Kim, G.H. Lee, E.S. Kim,S. Lee, S. Y. Lee, J. Hone,C. Lee, *Nanoscale*, 2013,**5**, 3063

Rahul S. Diggikar, Dattatray J. Late,
Bharat B. Kale

The unique morphologies of reduced graphene oxide (RGO) and RGO-PANI nanofibers (NF) composites have been demonstrated. The enhanced electrochemical performance was observed for honeycomb like RGO-PANI NFs composites.

